CHALLENGES WITH SHIP MODEL TESTS IN SHALLOW WATER WAVES

Manases Tello Ruiz[1]*, Marc Vantorre[1], Thibaut Van Zwijnsvoorde[1], Guillaume Delefortrie[2]

[1]Ghent University, Maritime Technology Division, Ghent, Belgium
[2] Flanders Hydraulics Research, Antwerp, Belgium

Manases.ruiz@UGent.be, Marc.Vantorre@UGent.be, Thibaut.VanZwijnsvoorde@UGent.be, Guillaume.Delefortrie@mow.vlaanderen.be

ABSTRACT

The new Energy Efficiency Design Index (EEDI) regulations issued by IMO consider among others ship manoeuvrability in adverse weather conditions. This has boosted research on ship manoeuvring in waves, which is being studied by different consortia in the world, e.g. SHOPERA [1] in Europe.

At the Towing Tank for Manoeuvres in Shallow Water [2] (co-operation Flanders Hydraulics Research – Ghent University) both captive and free running manoeuvring model tests in regular waves have been conducted in shallow water conditions. During the tests, different challenges were experienced, related to the ship motions, the wave behaviour in finite water depths, and the propagation of waves along the tank. In addition, challenges due to interaction between the ship, the waves, and the tank's sidewalls have also been encountered. In shallow water, such interaction is rather inevitable mainly due to the lower ship speeds attained. For this reason, tests with (regular) waves needed to be optimized according to several criteria. The publication provides an overview of these issues encountered and how these have been coped with in model testing.

1. OVERVIEW

Manoeuvring in waves has become one of the most important concerns for the research community motivated by the introduction of new regulations (EEDI) by IMO in 2013 to control CO_2 emissions by ships. These regulations limit the maximum installed power on board, which in turn raises questions regarding the ship's manoeuvring capability in adverse weather conditions. A distinction should be made between adverse weather conditions and extreme weather conditions. The former can also be associated to ship manoeuvring in moderate seas, as is the case in coastal areas when the ship approaches a port by access channels. In these regions the combination of waves, the restricted navigational area, and shallow water effects can lead to important limitation of manoeuvring capability of ships.

In shallow water (defined in [3] for ships by $h/T_m < 4$, and in [4] for waves by $kh < 1/10$, here h is the water depth, T_m is the mean draught and k is the wave number) additional effects on both the waves and the ship are observed; waves develop a nonlinear behaviour depending on their amplitude and period and ships undergo large hydrodynamic forces depending on their clearance between the bottom and the ship's keel (ukc). The additional forces in shallow water reduce the initial ukc (squat effect); hence, increasing the risks of bottom touch events due to the wave induced oscillations of the ship's keel.

To investigate wave effects on manoeuvring ships, model testing is still the most reliable method. For this purpose, at Flanders Hydraulic Research (FHR) experimental studies on

wave effects in shallow water have been conducted during the last years with three different ship models, the KVLCC2 (KRISO VLCC, designed by KRISO), the DTC (Duisburg test case, designed by the University of Duisburg-Essen), and a container ship hereafter named as C0W. The KVLCC2 and DTC ships were studied in the frame of the SHOPERA project while the C0W ship was the subject of an internal research project at Flanders Hydraulics Research (FHR).

Despite the advantages in using towing tank facilities, performing tests in shallow water is not straightforward. A first problem to be considered is bottom touch events; to avoid this, constraints for the ship vertical motions must be applied. Additionally, in a towing tank, tests in waves are also restricted by the limited tank's breadth; this as waves approaching the tank's side walls will be instantaneously reflected back to the ship, altering the initial (desired) wave environment. Moreover, for tests in regular waves, in [5] it is recommended to subject the ship to 10 wave cycles at least; this might not be an easy task to achieve as waves might not be stable along the tank. Hence, the behaviour of waves along the tank need to be also studied to ensure the ship is tested in a constant regular wave environment.

The challenges mentioned above have been studied for the three ship models mentioned earlier; their analysis has been done independently, but the procedure is similar for each ship model. In this work, the results and challenges encountered for the ship C0W (see Figure 2) are discussed. For such tests, the selected wave parameters are representative of the shallow waters encountered in the Belgian zone of the North Sea. During tests, the authors tried to comply with the deep water guidelines (see [5]) or adapt them whenever needed. To the authors' best knowledge, guidelines for model tests in shallow water waves have not been established yet.

2. EXPERIMENTAL PROGRAM IN SHALLOW WATER

2.1 Experimental setup, ship and numerical model

The experimental program was conducted in the Towing Tank for Manoeuvres in Shallow Water at FHR, Antwerp, Belgium. The towing tank's useful dimensions are 68 m by 7 m and the maximum water depth is 0.50 m. The towing tank carriage mechanisms consist of a main and a lateral carriage, and a yawing table. The main carriage moves in the longitudinal direction of the tank, the lateral carriage moves in the transversal direction, and a yawing table rotates the model in the horizontal plane (see Figure 1).

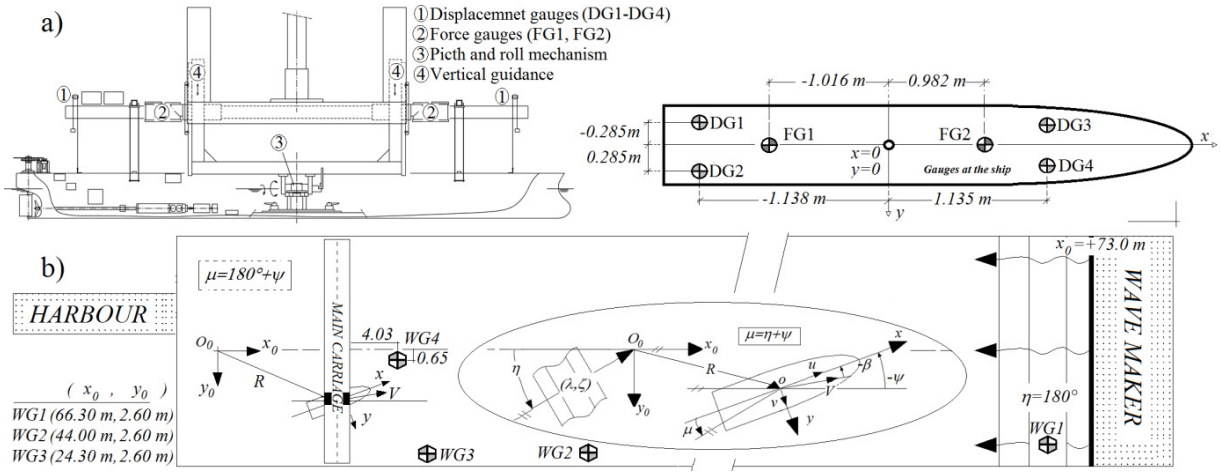

Figure 1 Towing tank at FHR, arrangement and setup for tests with and without waves

During captive tests a ship model is attached to the carriage mechanism, which can allow free heave, pitch and roll motions. The horizontal and lateral forces on the hull are measured by strain gauge dynamometers $FG1$ and $FG2$, the ship's vertical motions by potentiometers $DG1, DG2, DG3$ and $DG4$ (see Figure 1a), and the wave profile by resistance wires $WG1, WG2, WG3$ and $WG4$. The force gauges and displacement gauges were positioned in reference to the ship (see right in Figure 1a), while the wave gauges $WG1, WG2$ and $WG3$ were positioned relative to the towing tank (see Figure 1b). Only $WG4$ was attached to the main carriage at a distance as shown in Figure 1b.

The tests are defined by two coordinate systems (see Figure 1), the Earth bounded axes, $o_0 - x_0\ y_0\ z_0$ and the horizontal bound body fixed axes system, $o - xyz$, and both are North East down oriented. The longitudinal axis of the Earth axes system coincides with the towing tank's centre line and is positive towards the wave maker. For the body axis system, the longitudinal axis is aligned with the ship's centreline positive towards the bow when the ship is at rest. To define the ship's relative position during tests in waves, parameters such as wave angle of encounter μ, hull drift angle β, and ship's heading angle ψ are used. The wave angle relative to the Earth bounded axes is $\eta = 180°$. These definitions are sketched in Figure 1b.

The present study was conducted the ship C0W. The main characteristics are given in Table 1, and in Figure 2 a side and a profile view of the hull are presented.

Table 1 C0W ship main characteristics at full and model scale. Scale 1:90

$L_{PP}\ (m)$	$B\ (m)$	$T_m\ (m)$	Full scale	$L_{PP}\ (m)$	$B\ (m)$	$T_m\ (m)$	Model scale
377.2	56.4	15.282		4.191	0.627	0.1698	

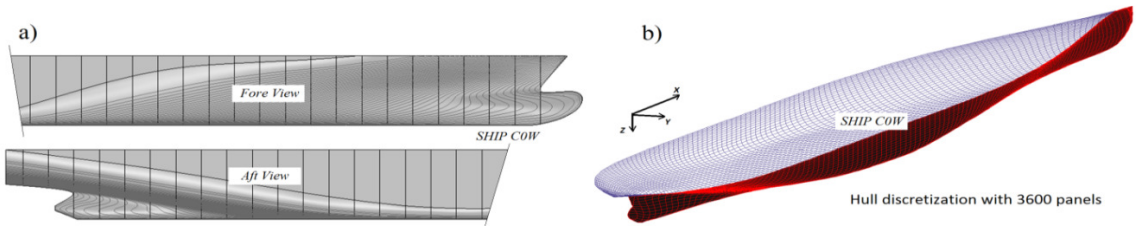

Figure 2 The ship C0W: (a) side view of the hull, and (b) Hydrostar hull discretization

In addition to the experimental study, a computation of the wave induced motion and forces have been conducted with the 3D potential panel method Hydrostar. Hydrostar uses the Green's function and the encounter frequency approximation, to compute the hydrodynamic forces with and without forward speed, see [6]. For the analysis of the ship C0W, first, a convergence analysis with a coarse, medium and a fine mesh was conducted. The final discretization with 3600 panels, for the entire hull (see Figure 2b), was selected.

2.2 Wave environment

The waves studied here are related to the Belgian zone of the North Sea (see Figure 3a). To gain a better idea on waves in this region, an example of the wave spectra is given in Figure 3b and, wave records in the Scheur/Wielingen region are presented in Table 2 in a form of a scatter diagram for the significant wave height (Hs) and the zero crossing wave period (Tz).

From Figure 3b, it can be observed that the spectra are concentrated in a range of frequencies situated between $\omega \approx 0.5$ and $\omega \approx 2\ rad/s$. Longer ($\omega < 0.5$) and shorter ($\omega > 2$) waves are still present but their energy density (S) is significantly smaller. From Table 2, it can be

seen that waves up to 2 m have a large probability to occur, P($Hs < 2\ m$) = 0.93, and if Hs is increased to 3 m this rises to P($Hs < 3\ m$)=0.99. For wave periods Tz up to 6.5 s a similar probability of 99% in found. This limit of $Tz = 6.5\ s$ does not imply that longer waves are absent, it only indicates that such waves have relative smaller amplitudes in contrast to shorter waves. This is a characteristic of coastal areas where short crested waves are predominant.

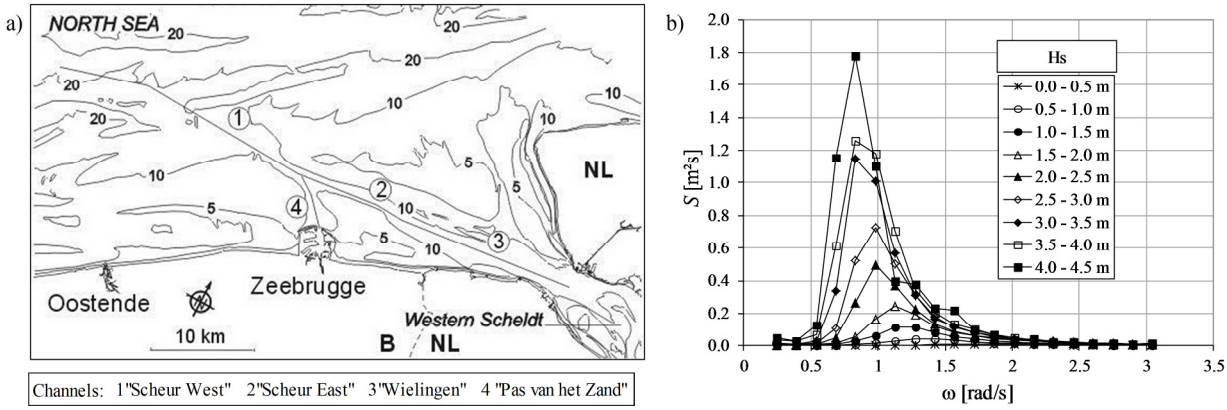

Figure 3 (a) Access channels to the mouth of the Western Scheldt and to Zeebrugge and, (b) Typical wave spectra in the Flemish Banks region [7]

Taking into account the stated above, a wave frequency range $\omega = 0.3$ to $\omega = 2.0\ rad/s$, and the wave height up to $H = 3\ m$ are chosen as limits for the main wave characteristics. To choose the final wave parameters, in addition to the limits established above, the ship needs to be considered as well. For the case of the C0W ship, the selected regular waves are presented in Table 3. In Table 3, in addition, the non-dimensional frequency ω' ($\omega' = \omega\sqrt{Lpp/g}$) and the wave length to ship length ratio λ/L_{PP} are also displayed.

Table 2 Scatter diagram of **Hs** and **Tz** near the Scheur/Wielingen channel [8]

Tz (s)	Hs (m) <=0.25	0.25 0.50	0.5 1.0	1.0 1.5	1.5 2.0	2.0 2.5	2.5 3.0	3.0 3.5	3.5 4.0	4.0 4.5	4.5 5.0	5.0 5.5	5.5 6.0	P(Tz)	P(≤Tz)
<=2.5	0.22	2.96	1.59	0.07	0	0	-	-	-	-	-	-	-	4.8	4.8
2.5 - 3.5	1.85	12.2	18.1	3	0.17	0.01	0	-	-	-	-	-	-	35.3	40.2
3.5 - 4.5	1.07	4.96	15.6	13.3	3.97	0.49	0.03	0.01	0	-	-	-	-	39.4	79.6
4.5 - 5.5	0.02	0.75	2.94	4.32	5.35	2.97	0.78	0.1	0.01	0	-	-	-	17.2	96.8
5.5 - 6.5	-	0.02	0.26	0.25	0.31	0.74	0.82	0.48	0.11	0.01	0	0	-	3.0	99.8
6.5 - 7.5	-	-	0	0.01	0	0.01	0.02	0.05	0.04	0.02	0	-	-	0.2	100.0
7.5 - 8.5	-	-	-	-	-	-	-	-	0	0	0	-	-	0.0	100.0
P(Hs)	3.2	20.9	38.5	21.0	9.8	4.2	1.7	0.6	0.2	0.03	0.0	0.0	0.0		
P(≤Hs)	3.2	24.0	62.5	83.5	93.3	97.5	99.1	99.8	99.9	100.0	100.0	100.0	100.0		

Table 3 Main wave parameters at full and model scale for a ship at **35%** $\boldsymbol{ukc}$. Scale 1:90

$\omega\ (rad/s)$	0.33	0.38	0.44	0.49	0.56	0.64	0.74	0.87	$h\ (m)$	$H\ (m)$
	Full scale								20.637	1.8 – 2.7
$\omega\ (rad/s)$	3.1	3.57	4.19	4.69	5.28	6.04	6.98	8.27	$h\ (mm)$	$H\ (mm)$
	Model scale								229.3	20 – 30
$\omega'\ (-)$	2.02	2.33	2.74	3.06	3.45	3.95	4.56	5.4	Scale	1:90
$\lambda/L_{PP}(-)$	0.7	0.6	0.5	0.44	0.38	0.32	0.26	0.2		

In Table 3 the wave frequency $\omega = 0.87\, rad/s$ has been set as an upper limit. A higher frequency has not been chosen because at $\omega = 0.87\, rad/s$ a ratio $\lambda/L_{PP} = 0.2$ is obtained, and it can be expected that at higher frequencies the ship will not be subjected to important wave effects. The lower limit, $\omega = 0.33\, rad/s$, differs slightly from the ones observed based on the energy spectrum. Lower frequencies than $\omega = 0.33\, rad/s$ still can be used for tests; however, such tests (at longer waves) will be rapidly contaminated by reflection from the towing tank's harbour, hence, they are avoided.

The selected waves shown in Table 3 have two different wave heights $H = 1.8\, m$ and $H = 2.7\, m$. These magnitudes are approximately the mean of the range of significant wave heights, $1.5 < Hs < 2.0\, m$, and $2.5 < Hs < 3.0\, m$. The larger wave height is chosen only to study the wave behaviour along the towing tank. The chosen wave heights are obtained based on the significant wave heights, in reality, smaller magnitudes are expected in the Belgian coastal waters. However, such waves cannot be used for model tests with ship COW because at the given scale factor wave effects will be very small and difficult to measure.

Keeping the wave height constant for varying periods, however, is not a standard procedure. In [5] it is recommended to keep a constant steepness H/λ to disregard the wave amplitude influence. This is not possible in shallow water, because, if the wave steepness is kept constant the resulting wave amplitudes for the longer waves (smaller wave numbers k) will be unrealistic for the Belgian coastal waters (see Figure 3b).

3. SHALLOW WATER PROBLEMS FOR TESTS IN WAVES

3.1 Wave behaviour in finite water depths

The behaviour of waves traveling along the tank has been investigated by generating wave trains and measuring them along the towing tank. For these tests, the lateral position of wave gauges $WG1$, $WG2$, and $WG3$ has been set to the tank's centre line ($y_0 = 0$) while keeping the longitudinal position as shown in Figure 1. The wave parameters are shown in Table 3. Bear in mind, that for these tests a wave height of $H = 30\, mm$ has been used.

In Figure 4 an example of the recorded data is presented for two different wave frequencies, $\omega = 8.27$ and $4.19\, rad/s$. The wave records measured by three wave gauges located along the tank are presented as function of time. For a better visualisation, the recorded data at $WG1$ and $WG3$ have been offset by a distance of $+20\, mm$ and $-20\, mm$, respectively.

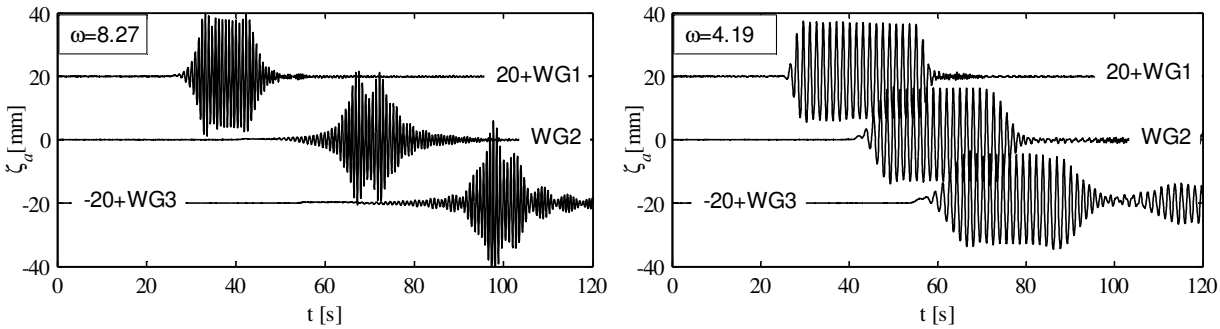

Figure 4 Wave records at $WG1$, $WG2$ and $WG3$, for a wave height $H = 30\, mm$

To examine the main wave characteristics, first a time window is selected from the recorded data, then a Fourier analysis is performed by fitting the data to Eq. (1) using a least square method to obtain the eight unknown parameters ($a_0, a_1, b_1, a_2, b_2, a_3, b_3, \omega$).

$$f(t) = a_0 + a_1\cos(\omega t) + b_1\sin(\omega t) + a_2\cos(2\omega t) + b_2\sin(2\omega t) + a_3\cos(3\omega t) + b_3\,sin(3\omega t) \quad (1)$$

The amplitudes of the first and second harmonics, resulting from the analysis, are plotted in Figure 5a against their fundamental frequency ω. A sample of the numerical fitting is shown in Figure 5b. In Figure 5a, the amplitudes of the mean and the third harmonic are not presented because they are significantly smaller (see Figure 5b).

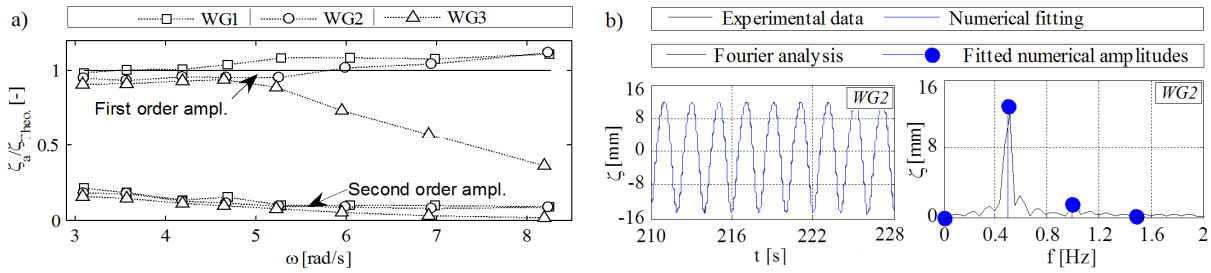

Figure 5 Regular waves along the tank. (a) First and second harmonic amplitudes, and (b) example of numerical fitting analysis

In general, for all wave frequencies it is observed that the first order values measured at $WG1$ and $WG2$ correspond with the desired wave amplitude $\zeta_a = 15\,mm$ $(H = 30\,mm)$, see Figure 5a. A slightly better agreement is observed for longer waves than for shorter waves. Such difference, however, can be corrected if the wave maker calibration is adjusted for shorter waves. This seems irrelevant in contrast to the decreasing magnitudes of the first order quantities observed at WG3; for shorter waves, their amplitude is reduced dramatically as the wave frequency increases. A possible explanation is the energy dissipation caused by the tank walls which will be stronger for shorter waves.

The second order magnitudes for all wave frequencies are in general less than 20% of the first order quantities, see Figure 5a. Such smaller values, together with the observed magnitudes for the first order components, suggest that these waves could be treated as linear until the location of $WG3$ for longer waves and $WG2$ for shorter waves. Hence, for tests in waves a meeting region can be defined where the evolution of waves is stable along the tank.

An additional problem is the occurrence of reflection from the harbour. This is avoided by defining a time interval calculated assuming pure reflection. For this time interval, the average speed of wave long the tank was used. This speed was obtained by dividing the distance between the wave gauges and their time difference between their first registered regular wave.

3.2 Ship motion constraint in shallow water

Considering the ship as a rigid body with linear harmonic motions, with rotation $\vec{\Omega} = (\xi_4, \xi_5, \xi_6)$ and translation $\vec{\mathrm{R}} = (\xi_1, \xi_2, \xi_3)$ with respect to the x, y, z coordinates. Here, $\xi_1, \xi_2, \xi_3\ \xi_4, \xi_5, \xi_6$ are the surge, sway, heave, roll, pitch, and yaw respectively. The displacement of any point is given by:

$$\vec{\xi}_{\vec{r}} = \vec{\mathrm{R}} + \vec{r} \times \vec{\Omega} \quad (2)$$

The motion components for the absolute displacement vector $\vec{\xi}_{\vec{r}} = (X_P, Y_P, Z_P)$ at any point $P = (x_P, y_P, z_P)$ with coordinates $\vec{r}$, are given by:

$$\begin{aligned} X_P &= \xi_1 + z_P\xi_5 - y_P\xi_6 \\ Y_P &= \xi_2 + x_P\xi_6 - z_P\xi_4 \\ Z_P &= \xi_3 + y_P\xi_4 - x_P\xi_5 \end{aligned} \tag{3}$$

The amplitude Z_P^a of the vertical displacement Z_P, considered as a linear harmonic motion and evaluated at the ship's centre line ($y_p = 0$), is then given by:

$$Z_P^a = \sqrt{(\xi_3^a)^2 + (x_P\xi_5^a)^2 - 2x_P\xi_3^a\xi_5^a\cos(\theta_5 - \theta_3)} \tag{4}$$

Here, θ_3, and θ_5, are phase angle for the ship motions in heave and pitch, respectively.

This motion amplitude Z_P^a of a point P in the ship is important because it reduces the distance between the ship's keel and the tank's bottom (ukc), hence, its prior evaluation is needed to avoid bottom touch events. To obtain Z_P^a, first, the ship motion responses are required. For the ship C0W, these numerical computations at full scale, $20\%\, ukc$, in head and following waves, and at two different forward speeds have been carried out in Hydrostar. The reduction in ukc due to wave induced motions is estimated by evaluating Z_P^a at a critical point, in here, a point located at the bow with coordinates $(0.5L_{PP}, 0,0)$ is considered.

The estimation of the local ukc reduction based only Z_P^a in shallow water is insufficient. In such scenarios accounting for squat effects is important. From the results presented in [9], a clearance reduction around $1\ m$ for a ship's speed of 12 knots can be used as a critical value, at lower speed the squat effect is expected to be less significant. The resulting reduction in ukc is depicted by the obtained vertical amplitudes Z_P^a at the point $(0.5L_{PP}, 0,0)$, and the squat effect. These are presented in Figure 6. In Figure 6 the shaded area correspond to the wave frequencies selected for the study of the C0W ship.

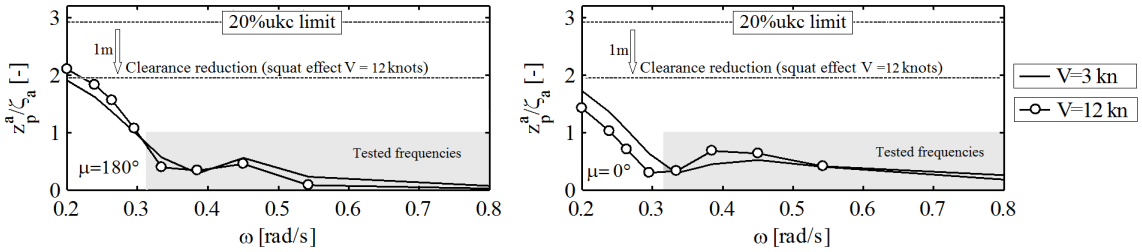

Figure 6 Z_P^a amplitudes for the C0W ship at two ship speeds $V = 3$ and 12 knots, and in head (left) and following (right) waves. ukc reduction due to squat, shown in dashed lines

The vertical responses show a maxima at frequency $\omega = 0.2$ rad/s, taking this value as a reference, a $1\ m$ wave amplitude and the reduced ukc due to squat, bottom touch events will occur in head waves for a ship speed of 12 knots. However, if now the selected wave frequencies described in Table 3 are considered (shaded area in Figure 6), the limiting $1\ m$ wave amplitude can be increased up to $2\ m$ which in turns implies a $4\ m$ wave height, such values are large value for coastal waters such as the Belgian zone of the North Sea. Hence, for the chosen wave characteristics, tests with the ship C0W ($H = 1.8\ m$ see Table 3) will not suffer from bottom touch events.

3.3 Tank sidewalls interaction

Ship model tests in waves in narrow tanks will suffer interaction with the tank's side walls. Such interaction occurs because the ship diffracts the incoming waves, and also due to the radiated waves generated by the ship motions. Such waves will travel forth and back to the

ship, hence, distorting the initial wave environment. This type of interaction cannot be totally neglected, yet, it is possible to minimize its effects. Considering tests in head or following waves, the interaction associated to the diffraction problem can be considered as minimal. Hence, to minimize the total interaction problem, the effects associated to the radiation need to be minimized. For such straight course tests, this is obtained by establishing a minimum (critical) forward speed. This speed, as described in [10], can be obtained by equating the time t_r the radiated waves travel a distance equal to the tank's breadth B_T and the time t_s the ship needs to advance one ship length L_{PP}.

$$t_r = \frac{B_T}{C_r}; \quad t_s = \frac{L_{PP}}{V} \quad \text{and} \quad C_r = \frac{g}{\omega_r} tanh(k_r h) \tag{5}$$

Here, V is the ship speed, C_r is the phase speed and ω_r is the frequency of the radiated waves, h is the water depth, and μ is the wave angle of encounter. The frequency of the radiated waves in here is equal to the encounter wave frequency $\omega_r = \omega_e = \omega - kVcos(\mu)$.

For deep water scenarios, the simplification of the dispersion relationship helps to find a formulation which expresses the critical speed as function of the wave frequencies for any B_T/L_{PP} ratio, see [5, 10]. For intermediate water, a function as such is not directly possible because the interdependence between the wave frequency and the wave number. However, through an iterative calculation using Eq. (5), it is yet possible to find the critical speed.

For the C0W model and the towing tank at FHR, ratio $B_T/L_{PP} = 1.67$, the critical speeds are found for head and following waves, at 50% and $100\%\, ukc$ (see Figure 7a). These limiting speeds are expressed non-dimensionally as Froude numbers and are plotted as a function of a non-dimensional frequency ω' ($\omega' = \omega\sqrt{Lpp/g}$). In Figure 7 the shaded area corresponds to the wave frequencies used in the study of the ship C0W.

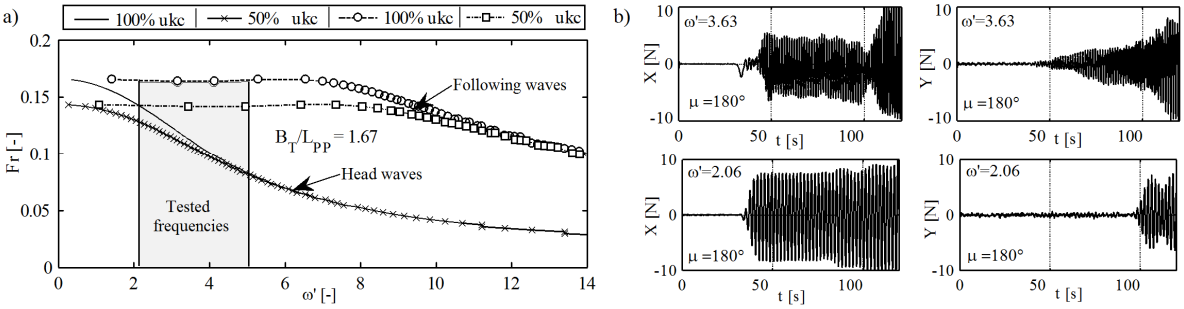

Figure 7 (a) Critical speed for the ship C0W, and (b) measured surge and sway forces at zero speed, $100\%\, ukc$, $\omega' = 3.63, \zeta_a = 32.8\, mm$ (top) and $\omega' = 2.06, \zeta_a = 10.1\, mm$ (bottom)

To illustrated the interaction with the tank's side walls, the measured forces for surge and sway obtained for the critical scenario of zero forward speed are presented in Figure 7b. Test conditions are: head waves, $100\%\, ukc$, two regular waves $\omega' = 3.63$, $\zeta_a = 32.8\, mm$ and $\omega' = 2.06$, $\zeta_a = 10.1\, mm$. These tests do not correspond to the selected waves in Table 3, but they have been conducted at FHR with the ship C0W.

From Figure 7a, smaller magnitudes for the critical speed can be observed for shallower water depths, $50\%\, ukc$ in contrast to $100\%\, ukc$, for both head and following waves. This lower limit is obtained because the maximum speed of waves propagating in shallow water is limited by $\sqrt{gh}$. The limited speed of waves in shallow water, on the other hand, helps to delimit the range of ship speeds under which interaction occurs for tests at lower wave

frequencies. Hence, in principle, it is possible to set ship speeds above the critical ones where all tests are free of interaction, see Figure 7a. For the ship C0W speeds equal or above $17\ knots$ ($F_r \approx 0.15$) could be selected. However, such magnitudes are considered as higher speeds for a ship navigating in shallow waters, and are not a common practice.

Considering the ship navigating in shallow water, it is clear that interaction will be always present for tests in following waves. This is not case for tests in head waves where is yet possible to obtain combinations of wave frequencies and ship's speeds free of interaction. For instance, for the frequencies used to test the ship C0W, the critical speeds wary between $15\ knots$ ($F_r \approx 0.125$) at $\omega' = 2.06$ and $9\ knots$ ($F_r \approx 0.075$) at $\omega' = 5.4$ (see Figure 7a), hence, tests at speeds slightly above these limits will be free of interaction.

Tests at zero forward speed are expected to be strongly affected by interaction with the tank's side walls. However, such effects might not be necessarily significant. This can be seen in Figure 7b when comparing the measured surge and sway forces obtained from tests at two different frequencies. In Figure 7b (top) surge and sway forces developed simultaneously, while in Figure 7b (bottom) significant sway forces are measured long after significant surge forces are measured. The simultaneous development of surge and sway forces in Figure 7b (top) reveals the presence of a transverse wave system, such waves can be only addressed to the radiated waves being reflected by the tank's side walls.

The different behaviour observed in Figure 7b (bottom), where interaction is less significant, could be addressed to lower frequency of excitation, or due to the smaller wave amplitude. To investigate this further, the results obtained from tests with the ship C0W at $35\%\ ukc$, and a forward speed of $3\ knots$ ($Fr = 0.025$) are analysed. To establish the importance of interaction effects, a different approach than the one used above is chosen. The heave and pitch motions, obtained experimentally and numerically, are compared. The numerical study (obtained from Hydrostar) does not account for side wall effects.

To compare the experimental and numerical results, first, the heave and pitch time series are analysed in a similar process as conducted for waves in subsection 3.1. However, in this case Eq. (1) is used up to second order with five unknowns ($a_1, b_1, a_2, b_2, \omega$). The amplitudes for the first and second harmonics are plotted in Figure 8 against their fundamental frequency ω.

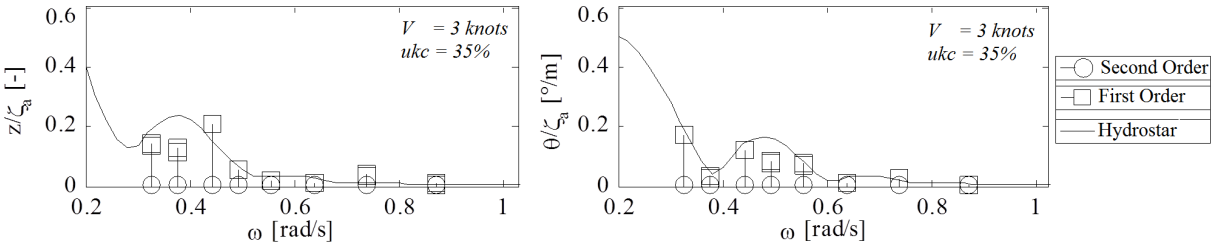

Figure 8 Motion responses for heave and pitch at $V = 3kn$ in head waves at $35\%\ ukc$

The smaller magnitude of the second harmonics observed in Figure 8 indicates that the motion responses in heave and pitch are mostly linear. Such smaller magnitudes support the comparison of the first order quantities against numerical results. The fair agreement between the experimental and numerical results, observed in Figure 8, indicates a lower influence of the tank's side walls effect in the heave and pitch motions. Some discrepancies are observed but they cannot be totally addressed to interaction effects or to uncertainties in the results. Determining the uncertainties at low speeds is not a straightforward process; this analysis is not considered in the present study but will be studied in further works.

4. CONCLUSIONS

Challenges related to the ship model tests in shallow water waves have been investigated. The wave behaviour along the tank, the induced ship motions, as well as interaction problem with the tank's side walls have been identified as main constrains. To study these challenges, tests have been conducted at FHR with the model of a container ship C0W in shallow water waves; the selected waves were representative of the Belgian coastal waters.

It has been found that waves along the tank behave different, for shorter waves a dissipation of their energy has been observed as they propagate along the tank. Tests at such frequencies, however, can still be used by defining a region along the tank where all waves are stable. Regarding the concerns of bottom touch events due to wave induced motion, it has been observed that they represent a less significant problem for relative larger under keel clearance ($ukc > 20\%$). However, their correct estimation will be more important for smaller ukc because at such clearances squat effects are stronger, hence, wave induced motions (even if they are small) could lead to bottom touch events. With regards to interaction with the tank's side walls, such effects will be always present in following waves due the limited speed of ships in shallow water. However, for tests in head waves, a limited combination of wave frequencies and ship speeds free of interaction is yet possible to obtain. It has also been found that even though interaction is present, if wave heights and ship motions are small, its effect on the heave and pitch motions can be neglected.

REFERENCES

1. SHOPERA. (2013-2016). *www.shopera.org*
2. Delefortrie, G., Geerts, S., and Vantorre, M. (2016) The towing tank for manoeuvres in shallow water. *MASHCON 2016*. Hamburg, Germany.
3. ITTC. (2014) Recommended procedures and guidelines, captive model test procedures (7.5-02-06-02).
4. Dean, R.G., and Dalrymple, R.A. (1991) Water wave mechanics for engineers and scientists. *World Scientific*.
5. ITTC. (2008) Testing and extrapolation methods, loads and responses, seakeeping, seakeeping experiments (7.5-02-07-02.1).
6. Bureau Veritas. (2012) HYDROSTAR for experts user manual.
7. Vantorre, M., and Journee, J. (2003) Validation of the strip theory code SEAWAY by model tests in very shallow water, *Report 1373-E, Delft University of Technology/SHL.*
8. Flemish Banks Monitoring Network. (1984-2004) *www.meetnetvlaamsebanken.be*
9. Vantorre, M., Laforce, E., Eloot, K., Richter, J., Verwilligen, J., and Lataire, E. (2008) Ship motions in shallow water as the base for a probabilistic approach policy. *OMAE*2008, pp.1–10.
10. LLoyd, A.R.J.M. (1989) Seakeeping: ship behaviour in rough weather. *Ellis Horwood*.

ACKNOWLEDGEMENTS

The present work is performed in the frame of project WL_2013_47 (Scientific support for investigating the manoeuvring behaviour of ships in waves), granted to Ghent University by Flanders Hydraulics Research, Antwerp (Department of Mobility and Public Works, Flemish Government, Belgium). For the numerical calculations a Hydrostar licence was put at the main author's disposal by Bureau Veritas through their Antwerp and Paris offices, which is highly appreciated.